Available online at www.sciencedirect.com

SCIENCE DIRECT®

ELSEVIER

Earth and Planetary Science Letters 215 (2003) 379–394

EPSL

www.elsevier.com/locate/epsl

Early Permian Pangea 'B' to Late Permian Pangea 'A'☆

Giovanni Muttoni [a,*], Dennis V. Kent [b,c], Eduardo Garzanti [d], Peter Brack [e], Niels Abrahamsen [f], Maurizio Gaetani [a]

[a] *Dipartimento di Scienze della Terra, Università di Milano, via Mangiagalli 34, 20133 Milan, Italy*
[b] *Lamont-Doherty Earth Observatory, Palisades, NY 10964, USA*
[c] *Department of Geological Sciences, Rutgers University, Piscataway, NJ 08854, USA*
[d] *Dipartimento di Scienze Geologiche e Geotecnologie, Università di Milano-Bicocca, Piazza della Scienza 4, 20126 Milan, Italy*
[e] *Departement Erdwissenschaften, ETH-Zentrum, CH-8092 Zürich, Switzerland*
[f] *Department of Earth Sciences, Aarhus University, Aarhus, Denmark*

Received 28 January 2003; received in revised form 16 May 2003; accepted 28 July 2003

Abstract

The pre-drift Wegenerian model of Pangea is almost universally accepted, but debate exists on its pre-Jurassic configuration since Ted Irving introduced Pangea 'B' by placing Gondwana farther to the east by ~3000 km with respect to Laurasia on the basis of paleomagnetic data. New paleomagnetic data from radiometrically dated Early Permian volcanic rocks from parts of Adria that are tectonically coherent with Africa (Gondwana), integrated with published coeval data from Gondwana and Laurasia, again only from igneous rocks, fully support a Pangea 'B' configuration in the Early Permian. The use of paleomagnetic data strictly from igneous rocks excludes artifacts from sedimentary inclination error as a contributing explanation for Pangea 'B'. The ultimate option to reject Pangea 'B' is to abandon the geocentric axial dipole hypothesis by introducing a significant non-dipole (zonal octupole) component in the Late Paleozoic time-averaged geomagnetic field. We demonstrate, however, by using a dataset consisting entirely of paleomagnetic directions with low inclinations from sampling sites confined to one hemisphere from Gondwana as well as Laurasia that the effects of a zonal octupole field contribution would not explain away the paleomagnetic evidence for Pangea 'B' in the Early Permian. We therefore regard the paleomagnetic evidence for an Early Permian Pangea 'B' as robust. The transformation from Pangea 'B' to Pangea 'A' took place during the Permian because Late Permian paleomagnetic data allow a Pangea 'A' configuration. We therefore review geological evidence from the literature in support of an intra-Pangea dextral megashear system. The transformation occurred after the cooling of the Variscan mega-suture and lasted ~20 Myr. In this interval, the Neotethys Ocean opened between India/Arabia and the Cimmerian microcontinents in the east, while widespread lithospheric wrenching and magmatism took place in the west around the Adriatic promontory. The general distribution of plate boundaries and resulting driving forces are qualitatively consistent with a right-lateral shear couple between Gondwana and Laurasia during the Permian. Transcurrent plate boundaries associated with the Pangea transformation reactivated Variscan shear zones and were subsequently exploited by the opening of western Neotethyan seaways in the Jurassic.

* Corresponding author. Tel.: +39-02-503-15518; Fax: +39-02-503-15494.
E-mail address: giovanni.muttoni1@unimi.it (G. Muttoni).

☆ Supplementary data associated with this article can be found at doi:10.1016/S0012-821X(03)00452-7

0012-821X/03/$ – see front matter
doi:10.1016/S0012-821X(03)00452-7

Keywords: paleomagnetism; Permian; Southern Alps; Pangea

1. The Pangea controversy

The Wegenerian configuration of Pangea, also known as Pangea 'A', is the widely accepted paleogeographic scenario in the Early Jurassic just prior to opening of the North Atlantic [1]. The earlier history of Pangea in the Late Paleozoic is, however, still debated since the introduction of the Pangea 'B' model by Irving [2] after pioneering analysis by Van Bemmelen and colleagues in the 1960s (see p. 109 in [1]). A recent paleomagnetic analysis concluded that a substantial amount of overlap of continental crust would have occurred in the Early Permian between Gondwana and Laurasia if reconstructed in a Pangea 'A' configuration [3]. The overlap could be eliminated by sliding Gondwana along lines of latitude to the east with respect to Laurasia, which would maintain the coherence of the paleomagnetic poles. This modification results in a Pangea 'B' configuration essentially identical to [2], which markedly differs from the Wegenerian Pangea 'A' and places South America (and Africa) adjacent to the southern margin of Europe. According to [3], Pangea 'B' transformed into Pangea 'A' essentially by the end of the Permian, and not in the Triassic as proposed by [2,4].

It is fair to say that Pangea 'B' and its tectonic implications have not been widely accepted by the earth sciences community. Various combinations of the following main arguments have been alternatively invoked to explain away the paleomagnetic evidence that has consistently resulted in a crustal misfit if a Pangea 'A' configuration is maintained in especially the Early Permian:

1. several paleomagnetic data from Gondwana are of poor quality, were retrieved from poorly dated rocks (e.g., continental redbeds from South America and Africa), or their ages underwent (sometimes unnoticed) reassessment [1,5];
2. the use of data with higher quality and better age constraints from (unrotated parts of) Adria as proxy for Africa [3] may be invalidated by tectonic decoupling of Adria and Africa during the Cenozoic Alpine orogeny [4];
3. an unrecognized contribution from a non-dipole field component (i.e., a zonal octupole of the same sign as the axial dipole) may have contaminated the geocentric axial dipole (GAD) field in the Late Paleozoic, making the crustal misfit at the basis of the Pangea 'B' model an artifact of an incomplete field model [6,7];
4. potential inclination error in sediments may produce paleolatitude artifacts virtually identical to those produced by an unrecognized zonal octupole contamination [5];
5. "there is no plausible geological evidence that would account for a megashear system of such magnitude" opined [8], referring to the Pangea 'B' to Pangea 'A' transformation assuming that it occurred in the Triassic [2,4].

2. Rationale

We contribute to a possible resolution of the Pangea conundrum by addressing the points listed above as follows:

1. the general paucity of reliable paleomagnetic data with good age control from Gondwana prompted us to retrieve new data of good quality and with good age control from Gondwana, as well as to focus our analysis on published data with quality factor (Q) ≥ 3 [1];
2. data from this study are from radiometrically well-dated Lower Permian rocks from relatively unrotated regions of Adria, i.e., the African promontory [9]. In response to concerns about the tectonic stability of unrotated portions of Adria, we further substantiate the well-known coherence between unrotated Adria and Africa paleomagnetic data for the Late Paleozoic, Mesozoic and Cenozoic;
3. data from Gondwana and Laurasia used in

this study have a narrow range of negative paleomagnetic inclinations of Kiaman age, which implies a narrow band of shallow paleolatitudes all comprised within one hemisphere. This greatly reduces the possible effects of any zonal non-dipole (e.g., octupole) field contamination [6,7] on Pangea geometry;

4. data from this study are from volcanic rocks and are compared with coeval data from the literature from Gondwana and Laurasia again strictly from well-dated volcanic rocks. This dataset thus virtually eliminates contamination of paleolatitudes by inclination error, which may occur in sediments but is hardly likely in volcanic rocks [5,6];
5. we present geologic and tectonic evidence in support of an intra-Pangea megashear that occurred, according to paleomagnetic data, within the Permian, after the Variscan orogeny but prior to the Triassic.

3. Adria contribution to Gondwana APWP

The crustal misfit at the basis of the Pangea 'B' solution was variably proposed to have existed in the Permian–Triassic [2], Early Permian [3] and Late Permian–Triassic [4]. Therefore, the Permian is a critical period of time for understanding the evolution of Pangea. Unfortunately, most Permian paleomagnetic data from Gondwana are from poorly dated clastic sedimentary successions in Africa and South America [1,4,10]. Focusing on volcanic rocks to avoid potential inclination errors in sediments would leave the Gondwana apparent polar wander path (APWP) with only two entries with $Q \geq 3$.

In order to augment the definition of the Gondwana APWP over the Early Permian, we adopt data from unrotated regions of Adria as proxy data for Gondwana. The reasons that motivated us to focus on Adria are: (i) unrotated portions of Adria are tectonically coherent with Africa; (ii) radiometrically well-dated volcanic rocks are available for sampling; (iii) there is good geological control of sampling sites in the Southern Alps.

Inspection of the structural setting (Fig. 1) reveals that the Adriatic foreland of Istria, Gargano, Apulia and Iblei has not yet been affected by Cenozoic Apenninic compression, which caused extensive differential rotations of thrust sheets in the Apennines [11]. The African affinity of these unrotated remnants of the Adria margin, as well as of specific regions of the thrusted margin of Adria such as the Adige/Dolomites, has been observed by many authors on the basis of geologic and paleomagnetic data [3,9,12–15]. Coherence of paleomagnetic poles from individual studies is evident, within typical resolution of a few degrees, for the Middle Triassic (data from Libya and Dolomites [14]; Fig. 1a), Late Jurassic/Early Cretaceous (data from South Africa and Southern Alps [9,14]; Fig. 1b), Late Cretaceous (data from various Gondwana localities, Southern Alps, Istria, Gargano and Iblei [1,9,14]; Fig. 1c), and the Miocene–Pliocene (data from Africa and Iblei [1,14]; Fig. 1d). Satellite (GPS) data substantially confirm this hypothesis also for modern times, whereby southeastern Adria (including Istria, Gargano, Apulia and Iblei, and the Adriatic foreland in

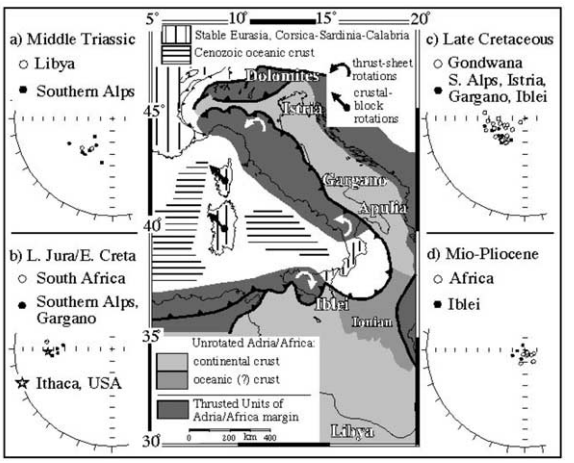

Fig. 1. Simplified tectonic map of Adria (central panel). 'Autochthonous' or unrotated regions that maintained tectonic coherence with Africa are distinguished from 'allochthonous' areas affected by thrust-sheet rotations. Panels a–d compare paleomagnetic poles from individual studies from the Southern Alps (essentially the Dolomites) and unrotated Adria (Istria, Gargano, Apulia and the Iblei) versus Gondwana from the Middle Triassic to the Mio–Pliocene (data from [1,9,14] and references therein). Fig. 5 documents such coherence also for the Early Permian.

general) is moving in conjunction with the African plate [16], whereas Apennine thrust sheets are moving eastward onto the undeformed Adriatic foreland [16] and rotating either counter-clockwise (e.g., Central–Northern Apennines [11,17]) or clockwise (Sicily) (Fig. 1).

The data from unrotated portions of Adria as proxy data for Africa are therefore not easily dismissible. The presumed discrepancy envisaged by [4] between the Late Jurassic/Early Cretaceous Adria paleopoles (Fig. 1b) and the coeval poles from conventional African APWPs [18] may derive from over-averaging many ill-defined paleopole entries from Africa, suppressing the information carried by one of the best-defined African poles, i.e., the Swartruggens kimberlite pole of [19]. This pole agrees with Adria data and supports a low latitude APW loop for Africa, as does another high quality pole, the Ithaca kimberlite pole of [20], when transferred into northwest African coordinates using the appropriate rotation parameters derived from the Central Atlantic magnetic anomalies (Fig. 1b).

4. Tectonic and stratigraphic setting of the Southern Alps

Permian volcanic rocks targeted by our analysis crop out in the Southern Alps (Fig. 2), which consist of a south-vergent thrust stack originating from N–S Alpine compression during the Cenozoic. Unlike the Adriatic foreland, thrust-sheet rotations cannot be excluded in the Southern Alps, especially in the vicinity of major fault/thrust systems. However, at our main sampling sites in the Adige Valley region as well as in the nearby Dolomites, Alpine faults border an area of relatively low upper crustal deformation (Fig. 2). Cenozoic tectonics disrupted locally and superficially the Upper Permian–Triassic succession [21] above the Lower Permian volcanic units sampled in this study, which remained coupled with their Variscan basement. At crustal scale, the Adige/Dolomites area shows a relatively simple tectonic structure involving a limited number of deep-seated thrusts with southward displacement of a few tens of kilometers, emerging to the surface in the highly deformed Insubric, Valsugana and Montello regions.

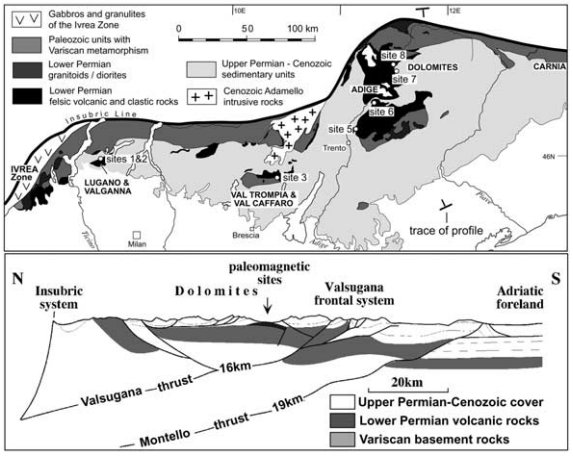

Fig. 2. Geologic sketch map of the Southern Alps with location of sampling sites (Table 1). Lower panel shows geologic cross-section across the Dolomites/Adige Valley region from the Insubric Line to the Adriatic foreland [21] with projected location of sampling area. The Valsugana and Montello deep-seated thrusts have total southward displacement of 16 and 19 km, respectively [21].

During the Early Permian, the Southern Alps experienced a post-Variscan phase of transtensional tectonics associated with widespread magmatism. Permian magmatic products are preserved as shallow intrusions, lavas, and up to 3 km thick volcano-sedimentary units that accumulated in rapidly subsiding troughs [22–24]. Trace element and isotope analyses indicate that magmas were produced by the interaction of mantle-derived melts with lower crustal rocks [24–26]. Rb–Sr age data on mica and whole rock are in the range 285–261 Ma [27]. However, recent U–Pb data on zircons [28] narrow the emplacement of the shallow intrusions and main volcanism to the Early Permian (284–276 Ma; Fig. 3). This tectono-magmatic event is post-Variscan because the cooling of the Variscan basement in the Southern Alps took place in the early Late Carboniferous (Rb–Sr data on biotite [28]; Fig. 3). The first unmetamorphosed sediments overlying Variscan metamorphic rocks are Westphalian E in age [29] (Logone and Manno conglomerates; Fig. 3).

The heterogeneous and laterally discontinuous

Lower Permian succession is overlain by Upper Permian post-tectonic fluviatile redbeds (~265–255 Ma; Verrucano Lombardo-Val Gardena lithosome). A syn- to post-Illawarra age (~265 Ma [30]) is assumed for the base of the Val Gardena Sandstone after magnetostratigraphic data [31].

Sampling for paleomagnetism (Fig. 2) was restricted to Lower Permian ignimbrites and lavas with direct or extrapolated age control (Fig. 3) and measurable bedding attitudes (Table 1, caption). Sites 1 and 2 were taken in the Lower Ignimbrite in Valganna, site 3 in the Lower Ignimbrite in Val Caffaro, site 5 in the Albiano Ignimbrite of Trentino, and sites 6, 7 and 8, respectively, in the Montan Ignimbrite, Thiesen Vitrophyre, and Lower Andesites in the Adige Valley (Table 1). Sites 1–3 are the only Southern Alps sites outside the Adige/Dolomites region. Although rigidly coupled with their Variscan basement, unlike in the Adige/Dolomites they bear a significant amount of tilting (Table 1, caption). By comparing data from within and outside the Adige/Dolomites, we can test the lateral consistency of the African paleomagnetic signature across the Southern Alps.

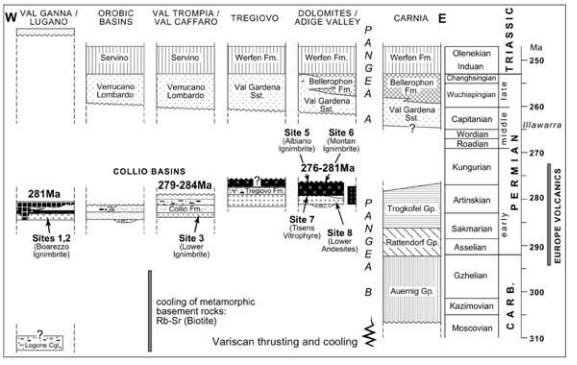

Fig. 3. Age and stratigraphy of Permian units in the Southern Alps with indication of sampling sites. The Permian part of this time scale is a close derivative of [82] with a modified age for the base of the Triassic after [83,84]. For the age of the Upper Carboniferous, we followed [30]. Range of cooling ages for the upper crustal basement of the Southern Alps are after [27,28].

Table 1
Paleomagnetic directions from Early Permian volcanics from the Southern Alps

Site	SLAT/SLONG	Locality	Unit	N	GDECL (°E)	GINCL (°)	α_{95} (°)	k	BDECL (°E)	BINCL (°)	α_{95} (°)	k
Site 1	45°54.8′N/8°49.2′E	Boarezzo, Valganna	Lower Ignimbrite	18	142.2	7.4	3.6	92	139.4	−31.9	3.6	92
Site 2	45°54.3′N/8°48.9′E	Boarezzo, Valganna	Lower Ignimbrite	23	146.7	3.5	3.0	104	147.8	−31.2	3.0	104
Site 3	45°50.3′N/10°27.2′E	~Bagolino, Brescia	Lower Ignimbrite	8	140.2	−25.5	6.7	69	146.3	−19.1	6.7	69
Site 5	~46°06.0′N/11°12.0′E	Albiano, Trentino	Albiano Ignimbrite	6	163.7	−21.9	1.8	1373	159.3	−14.8	1.8	1357
Site 6	~46°18.0′N/11°18.0′E	Rio Negro, Südtirol	Montan Ignimbrite	11	149.0	−27.5	4.1	128	155.1	−39.5	4.1	128
Site 7	46°34.7′N/11°32.1′E	Thiesen, Südtirol	Thiesen Vitrophyre	8	156.8	−17.4	2.5	511	160.4	−25.2	2.4	515
Site 8	46°34.3′N/11°31.6′E	~Thiesen, Südtirol	Lower Andesites	10	149.6	−7.1	4.8	102	151.3	−16.2	4.8	102
All sites	Southern Alps			7	149.7	−13.0	12.3	25	151.5	−25.6	8.6	50

Site: sampling sites in Fig. 2. SLAT/SLONG: latitude and longitude of sampling site; Locality and Unit: geographic locality and name of sampled volcanic unit; N: number of standard 11.4 cc specimens that yielded usable paleomagnetic directions; GDECL, GINCL, BDECL, BINCL: declination, expressed in °E, and inclination, expressed in °, of mean paleomagnetic direction in geographic (in situ) and bedding (tilt corrected) coordinates, respectively; k, Fisher precision parameter; α_{95}: Fisher radius of cone of 95% confidence about the mean direction. Bedding orientation of sampling sites (i.e., azimuth of bedding dip, expressed in °E, versus angle of bedding dip, expressed in ° with respect to horizontal): Site 1 158°E/41, Site 2 140°E/35, Site 3 30°E/16, Site 5 280°E/15, Site 6 115°E/15, Site 7 109°E/12, Site 8 109°E/12.

5. Paleomagnetism

Oriented paleomagnetic samples were collected with a petrol-powered rock drill at sites 1 and 2, whereas hand samples were taken at the remaining sites. From each 2.5 cm diameter core sample, one or two standard ~11 cc specimens were cut for magnetic measurements. The total number of sites/specimens analyzed is 7/89. All specimens were subjected to complete stepwise alternating field (AF) or, less frequently, combined AF and thermal demagnetization. Remanence measurements were performed on a Schonstedt spinner magnetometer, located in a magnetically shielded cage at Aarhus University. Least-squares line fitting [32] was used to determine the component directions in demagnetization intervals chosen by eye from orthogonal projections. Mean directions were calculated using standard Fisher statistics.

5.1. Rock magnetic properties

The magnetic mineralogy of selected samples from each site was inferred from isothermal remanent magnetization (IRM) experiments using the method of [33]. An IRM in 2.5 T was initially imparted along the sample $-z$-axis and was then progressively acquired along the sample $+z$-axis up to 2.5 T. Finally, a composite IRM at 2.5, 0.6 and 0.2 T fields was induced along sample orthogonal axes and thermally demagnetized, with measurements of the resultant remanence performed after each demagnetization step.

Samples from sites 1, 2 and 7 have IRM acquisition curves that approach saturation at fields of ~0.3 T. The thermal unblocking characteristics of orthogonal axes IRM show the presence of a dominant low coercivity ($\leq$0.2 T) magnetic phase with maximum unblocking temperatures of ~575°C (Fig. 4a). These observations suggest

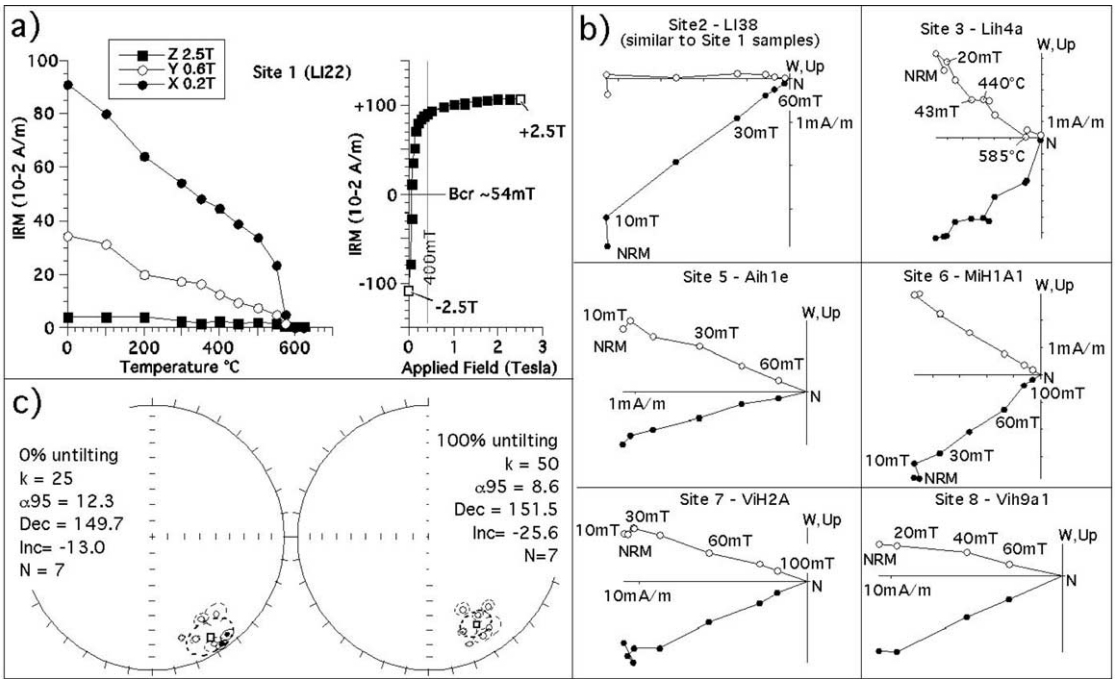

Fig. 4. Rock magnetic and paleomagnetic characteristics of selected samples from Lower Permian volcanic rocks from the Southern Alps. (a) A dominant magnetite phase is generally revealed by IRM acquisition curves and thermal unblocking characteristics of orthogonal axes IRMs [33]. (b) Vector end-point demagnetization diagrams show the occurrence of stable and generally univectorial characteristic components oriented to the south in geographic coordinates. Open/solid symbols are projections onto the vertical/horizontal plane. (c) Site mean characteristic component directions projected on an equal area stereonet. Open symbols represent negative inclinations.

that magnetite is the main carrier of the magnetic remanence at these sites. Sites 5 and 6 are also dominated by magnetite in association with subsidiary amounts of a higher coercivity/higher (~680°C) unblocking temperature phase interpreted as hematite. Sites 3 and 8 show a mixture of magnetite and hematite. At these sites, the percentage of the composite (total) IRM left after heating at 625°C is 38% (site 3) and 26% (site 8), and is almost entirely accounted for by the 2.5 T (i.e., ~hematite) magnetization component.

5.2. Paleomagnetic directions

Orthogonal projections of AF demagnetization data on magnetite-dominated samples indicate the presence of a stable magnetization component consistently oriented southeast and shallow-up (in geographic coordinates). This characteristic component is removed between ~10 mT and ~60 mT (up to a maximum of 100 mT) after elimination of an initial, highly scattered viscous overprint (Fig. 4b). Site 3 samples, bearing a mixture of magnetite and hematite, have been AF demagnetized up to 43 mT, and successively thermally demagnetized from 440 to 660°C. These samples show a component structure similar to samples dominated by magnetite. The small remanence left above 585°C is not associated with detectable changes in component direction.

The seven site mean characteristic component directions are relatively well-grouped in geographic coordinates. Upon application of full bedding tilt correction, the directions converge and the Fisher precision parameter k increases by a factor of 2 (Fig. 4c; Table 1), although the improvement is not statistically significant according to criteria of [34] because we chose to sample volcanic layers with least deformation and tilt. A peak in k was found at 70% untilting, with the overall mean direction displaced by only 3.8° from the overall direction at 100% untilting. However, this peak in grouping is not statistically significant and is moreover unlikely to be due to a syn-folding remagnetization. In fact, the overall mean direction at 70% untilting is far removed (~27°) from the Africa reference direction of Alpine Orogeny age [14] when overprinting might have occurred, whereas no evidence of tectonic displacement of such magnitude between unrotated Adria and Africa is available (see Section 4). We therefore attribute the peak in grouping at 70% untilting to a statistical artifact or perhaps to primary tilt of the ignimbrite layers.

The substantial grouping of paleomagnetic directions between sites up to 200 km apart indicates that Cenozoic Alpine deformation did not involve differential rotation of thrust sheets at our sampling localities within the Southern Alps. We attribute the observed characteristic magnetization component as representing a record of the Early Permian paleomagnetic field acquired during a radiometrically well-constrained portion of the Kiaman long reverse superchron (~284–276 Ma). The corresponding mean paleomagnetic pole (calculated at 100% untilting) is located at 236°E, 50°N ($dp/dm = 5°/9°$, $k = 50$; Table 2[1]).

6. Comparison with data from the literature

6.1. Data from Gondwana

The Early Permian (~284–276 Ma) paleomagnetic pole from this study compares favorably with previously published paleopoles from volcanic rocks from the Southern Alps with high quality factor ($Q \geq 3$ [1]; Fig. 5). These entries (items 2–7, Table 2[1]) come from rocks pertaining to the same volcanic cycle of this study and are of the same age.

The Southalpine poles agree with paleopoles from broadly coeval volcanic rocks from Morocco [35,36], the only two $Q \geq 3$ poles from volcanic rocks of comparable age from West Gondwana ([1]; Global Paleomagnetic Database 2003). These volcanic rocks, which accumulated in transtensional basins, are intercalated with continental sediments yielding Early Permian (Autunian) floras [37]. Importantly, the Moroccan paleomagnetic data were fully demagnetized and revealed a characteristic component of magnetization of reversed polarity probably acquired during the Kia-

[1] For Table 2 see online version of this article.

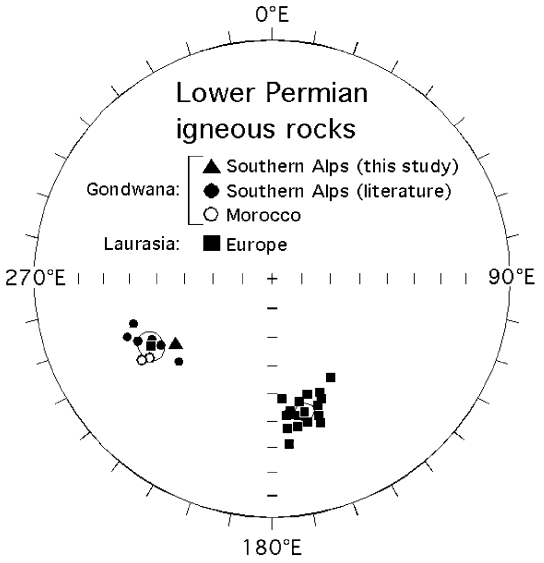

Fig. 5. Early Permian paleomagnetic poles from volcanic rocks from the Southern Alps and Gondwana compared with broadly coeval poles from Laurasia (Table 2[1]) with [1] quality factor $Q \geq 3$.

man reverse polarity superchron, or in any case not during the Cretaceous normal polarity superchron, as suggested for some other remagnetized Moroccan data [5].

The mean of the Moroccan poles (237.5°E, 37.5°N) lies within 6° of the mean Adria pole from coeval rocks (242°E, 43°N), suggesting that they belong to the same population (Fig. 5). This supports the tectonic coherence, within typical paleomagnetic resolution, of unrotated Adria regions and Africa during the Early Permian. Such coherence is also paleomagnetically valid for the Middle Triassic, Late Jurassic/Early Cretaceous, Late Cretaceous, and Miocene–Pliocene (Fig. 1), and is consistent with the southeastern Adria model of [16] as inferred from GPS velocities.

The tectonic coherence of Africa and Adria since the Early Permian allows us to calculate an overall mean Early Permian paleopole for Greater Africa, which is largely based on the ~284–276 Ma volcanics data from the Southern Alps and substantiated by the Moroccan data. This overall paleopole (41°N, 241°E, $A_{95} = 4.7°$, $k = 122$, $n = 9$; Table 2[1]) lies within 7° of the Early Permian paleopole for West Gondwana calculated by [1] from volcanics and redbeds (34°N, 242°E, $A_{95} = 7°$, $k = 60$, $n = 8$).

6.2. Data from Europe

The Early Permian collection of paleopoles from Europe as proxy for Laurasia (Table 2[1]) derives from [1] and the Global Paleomagnetic Database 2003. We used data with quality factor $Q \geq 3$ from magmatic rocks of known age pertaining to the Permian portion of the Permo–Carboniferous European magmatic province [38]. Paleomagnetic data that could not be confidently assigned an age estimate (by means of literature analysis) were rejected. The large majority of the data from this compilation were thoroughly demagnetized and are all invariably characterized by predominant reverse (i.e., Kiaman) polarity, consistent with maximum/minimum radiometric dates of ~294–273 Ma (Table 2[1]). Although some of these data were published in the 1960s and 1970s, the relatively high stability and intensity of the natural remanence characterizing these Permian volcanic rocks allowed them to be fully described with earlier laboratory techniques; in fact, recent studies have not altered the conclusions of older ones (Table 2[1]).

The overall mean Early Permian volcanics paleopole for stable Europe (42°N, 166°E, $A_{95} = 3.1°$, $k = 126$, $n = 18$; Table 2[1]) lies within 4° of the Early Permian paleopole for Laurasia calculated by [1] from volcanics and redbeds (45°N, 162°E, $A_{95} = 1.9°$, $k = 161$, $n = 35$).

7. The Early Permian Pangea 'A' misfit

The Wegenerian Pangea 'A' is a widely accepted paleogeographic scenario for coalescence of Gondwana with Laurasia in the Late Paleozoic to the opening of the Atlantic Ocean in the Jurassic. However, when used as a template to reconstruct Pangea 'A' in the Early Permian, the Africa and Europe mean Early Permian paleopoles outlined above would require a latitudinal overlap of over 1000 km between Gondwana and Laurasia that involves cratonic portions of both supercon-

tinents (Fig. 6), as already pointed out by [2]. Recently, two explanations have been put forward to explain the well-known paleolatitudinal misfit in order to maintain a Pangea 'A' model in the Early Permian.

7.1. Octupole contamination

Van der Voo and Torsvik [6] and Torsvik and Van der Voo [7] suggested that the observed Permo–Triassic paleolatitudes from Laurasia and Gondwana have been underestimated due to an uncompensated contribution from a long-term zonal octupole (G3) field. Paleomagnetic data used by [6] to reconstruct Pangea come mainly from non-equatorial regions of Laurasia in the northern hemisphere (e.g., central–northern Europe) and Gondwana in the southern hemisphere (e.g., Argentina, Tanzania). Such a distribution would amplify any G3 contamination of the GAD field that shallows inclinations, and hence paleolatitudes inferred from them (Fig. 7a), and thereby could artificially introduce a latitudinal overlap of Gondwana and Laurasia continental crust in equatorial regions (Fig. 6). A ~10% G3 contamination in the Permian was suggested by [7] although ~20% was required to fully explain the latitudinal misfit between Gondwana and Laurasia [6].

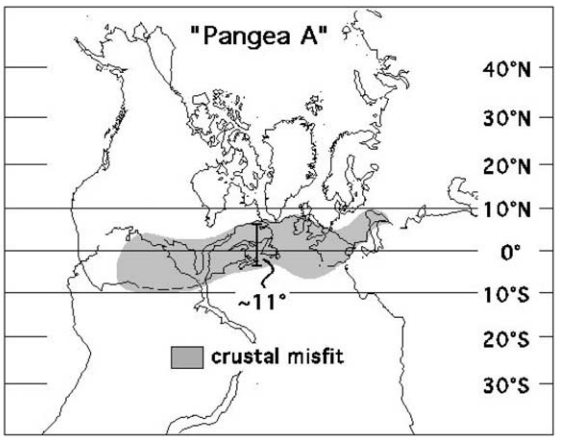

Fig. 6. The Early Permian overall mean paleopoles from Gondwana and Laurasia (Table 2[1]) produce a crustal misfit of more than 1000 km at tropical latitudes when used to reconstruct Pangea 'A'. See text for discussion.

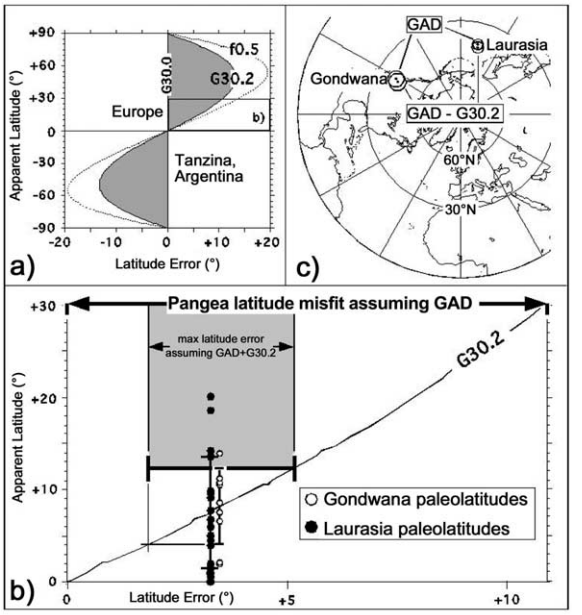

Fig. 7. (a) Apparent latitude and latitude error plotted with a 20% octupole (G30.2) contribution of the same sign added to the dipole field, as well as assuming an inclination error in sediments with flattening factor (*f*) of 0.5. (b) Enlargement of panel a showing that all paleomagnetic data from Gondwana and Laurasia of this study come from a narrow band of paleolatitudes from the northern hemisphere (Table 2[1], observed paleolatitudes). This distribution minimizes contamination of the GAD field by any G3 component (e.g., G30.2 is the 20% G3 suggested by [6]). Vertical bars on paleolatitude data are 2σ errors centered about the mean paleolatitude values. The long horizontal error bar is the total amount of crustal misfit between Gondwana and Laurasia in a 'Pangea 'A'' configuration as from Fig. 6, whereas the short horizontal error bar/shaded area represents the maximum amount of crustal misfit removable by assuming contamination of the GAD field by a 20% G3 component. (c) Polar projection of the Early Permian overall mean paleopoles of Gondwana and Laurasia plotted assuming a GAD field (Table 2[1]) and a GAD field contaminated by a ~20% G3 component, whose removal results in a northward displacement of only 2° of both Gondwana and Laurasia paleopoles (GAD−G30.2). See text for discussion.

All paleomagnetic data for both Gondwana and Laurasia used in this study, however, have low negative (Kiaman) paleomagnetic inclinations and therefore come from within a narrow band of paleolatitudes from the same (northern) hemisphere (Table 2[1]; Fig. 7b). Under such circum-

stances, accounting for a potential contamination of the GAD field by even a large ~20% G3 component sensu [6] would simply produce a negligible (~2°) northward displacement of both Gondwana and Laurasia while substantially maintaining their mutual misfit (Fig. 7c). Even using ad absurdum data located at the extremes of the paleolatitude distributions for Gondwana and Laurasia, less than one third (~3°) of the total amount of paleolatitude misfit can be accounted for by assuming a G3 contribution as much as 20% (Fig. 7b), which is in any case twice the amount of the Early Permian G3 estimate of [7].

In conclusion, as far as the Early Permian data of this study are concerned, the possible existence of a zonal octupole contamination does not explain satisfactorily the problem of the latitude misfit of Gondwana and Laurasia when reconstructed in a Pangea 'A' configuration.

7.2. Inclination error in sediments

Inclination error in sediments can produce a paleolatitude anomaly similar to the anomaly produced by contamination of the dipole field by a zonal octupole term [5]. Assuming a flattening factor (f) of 0.5 (Fig. 7a) for data from the Permian–Triassic sediments compiled by [4], Rochette and Vandamme [5] concluded that especially Gondwana sites located at (apparent) mid-paleolatitudes in the southern hemisphere could be affected by as much as ~20° of paleolatitude error.

Our study exclusively uses data from volcanic rocks, in which inclination error is not expected and in any case would be minimized at low inclinations. Therefore, as for the octupole hypothesis, we observe that inclination error in sediments does not explain the problem of the latitude misfit of Gondwana and Laurasia when reconstructed in a Pangea 'A' configuration using this study data.

8. Early Permian Pangea 'B' to Late Permian Pangea 'A'

The paleolatitudinal discrepancy between Gondwana and Laurasia that we obtain from a restricted (magmatic) dataset is similar to what has been found in many previous analyses and is evidently considered a persistent feature of the paleomagnetic data that has prompted several non-GAD explanations (e.g., G3 contamination of the GAD field or inclination error in sediments). We believe that the Early Permian magmatic paleopoles provide an accurate record of paleolatitudes using the GAD field model and thus require an adjustment to the Pangea paleogeographic model. Our solution to eliminate the crustal misfit uses the longitude indeterminacy of paleomagnetic data by sliding Gondwana to the east with respect to Laurasia (Fig. 8, upper panel). The resulting reconstruction of Pangea that satisfies the Early Permian magmatic paleopoles and eliminates continental overlap is essentially the same as Pangea 'B' of [2].

Muttoni et al. [3] showed that the reconstruction of Pangea that satisfies the Late Permian (and Early Triassic) Gondwana and Laurasia paleopoles is similar to Pangea 'A-2' of [39] (Fig. 8, lower panel). Therefore, we propose that the ~3000 km of dextral megashear between Gondwana and Laurasia occurred entirely within the Permian, from a Pangea 'B' configuration in the Early Permian to a Wegenerian-'A' configuration by the end of the Permian.

We suggest that the Pangea transformation began ~285 Ma after the Variscan Orogeny. Major tectonic features that we believe are closely associated with the initiation of the mid-Permian Pangea transformation include the initial opening of the Neotethys Ocean in the east between India/Arabia and the Cimmerian continents (e.g., Central Iran), and widespread lithospheric wrenching and magmatism in the west along the margin of the Adriatic promontory.

The eastern Neotethyan rift started in Early to Late Carboniferous times from Tibet [40] to Oman [41]. In the northwestern Himalaya, Neotethyan rifting reached its climax with the onset of bimodal volcanism and intrusion of alkali granites, dated radiometrically at 284 ± 1 Ma (U–Pb on zircons [42]), and biostratigraphically constrained to the earliest Permian [43,44]. Break-up and formation of oceanic crust followed shortly afterwards from the Himalayas all the way to

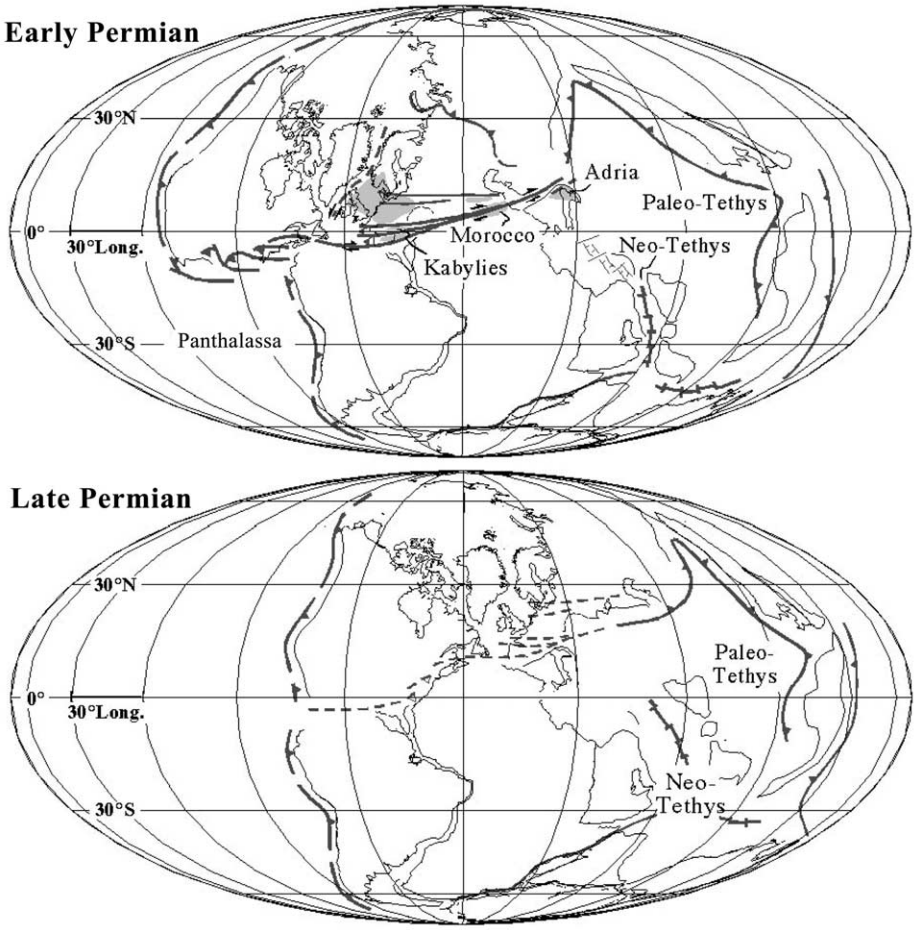

Fig. 8. The mid-Permian Pangea transformation from Pangea 'B' in the Early Permian to Pangea 'A' in the Late Permian. Africa is internally treated as three plates (NW, NE and S Africa), with Adria tectonically coherent with NW Africa. NW Africa and Adria are reconstructed using an Euler pole at 22.5°N, 158.5°E, Ω50.6° (obtained by multiplying the Euler pole derived from the paleomagnetic pole of Gondwana of Table 2[1] within error resolution with a pole located at 90°N with Ω ~ 20° to eliminate the continental overlap of Fig. 6). Internal Gondwana plates are reconstructed using Euler poles of [85]. Laurasia is reconstructed using an Euler pole located at 0°N, 78°E, Ω48° (obtained from the paleomagnetic pole of Laurasia of Table 2[1] within error resolution). Internal Laurasia plates are reconstructed using Euler poles of [86]. Tectonic lineaments are from [70,76]. Eastern Tethys blocks and circum-Tethys and circum-Pangea subduction zones are from [69].

northern Oman at mid-Early Permian times (mid-Sakmarian [45,46]).

To the northwest of Arabia, the lower crust and subcontinental mantle beneath the future outer continental margin of Adria were severely affected by extensional delamination and partial melting [47–49]. The Adriatic lower crust was intruded by gabbros in Early Permian times, from the Northern Apennines [50] to the Austroalpine Domain [51,52]. In the Southern Alps, the emplacement of mantle-derived mafic magmas at lower crustal levels occurred at 290–280 Ma (e.g., [53,54]). The ascent and emplacement of granitoid magmas in the upper crust was facilitated by deep-reaching transtensional faults [55,56]. At the surface, volcanic rocks and clastic sediments (e.g., Collio Basin: 284–279 Ma [28]) rapidly filled strongly subsiding strike-slip basins. This tectono-magmatic event was accompanied by andalusite-grade high temperature/low pressure metamor-

phism at mid-crustal levels along the northern margin of Adria, from Tuscany [57] to the Southalpine and Austroalpine Domains [58,59], reaching granulite facies in the lower crust [60].

8.1. Timing of the mid-Permian Pangea transformation

The mid-Permian Pangea transformation occurred in the Southern Alps well after the cooling of the Variscan basement, between the onset of lithospheric wrenching, subsidence of 'hot' strike-slip basins and volcanism (~285 Ma), and the deposition of Middle–Upper Permian post-tectonic redbeds (265–255 Ma; Fig. 3). The ~20 Myr stratigraphic gap separating the Lower Permian volcanic units (which rendered Pangea 'B' paleopoles) and the Middle–Upper Permian post-tectonic redbeds (which rendered Pangea 'A' paleopoles [3]) matches the timing of the envisaged transformation (Fig. 3; 'Palatinian Phase' of [23]). Sediment composition and geometry of the Middle–Upper Permian redbeds (Verrucano Lombardo-Val Gardena lithosome) suggests a gradual peneplanation of the source areas [61]. These terrigenous units testify to non-localized subsidence of a broad sedimentary basin [23,62]. Average rates of sediment accumulation (200–350 m deposited in ~10 Myr) were one order of magnitude smaller than in the Lower Permian troughs (1000–2000 m deposited in ~5 Myr). This suggests waning tectonic activity at the end of the Pangea transformation and the transition to a 'successor basin' setting characterized by lithospheric cooling. This stage of thermal relaxation is in line with the widespread occurrence of major transgressions in the late Middle Permian all along the newly formed Neotethyan passive margins, from northern India [45,63] to eastern Arabia [64,65] and in the Mediterranean region as well [23,66].

A similar evolution from Lower Permian deposition in 'hot' strike-slip basins with volcanism to deposition of post-volcanic redbeds in the Middle–Upper Permian after a significant mid-Permian unconformity occurred also in large portions of central Europe, e.g., in the Saar-Nahe basin [67] and in the NE German basin [68].

9. Driving forces and plate boundaries

Neotethyan rifting along the eastern margin of Gondwana and the subduction of Panthalassan oceanic crust underneath the western margin of Gondwana [69] provided the 'push-pull' driving force couple for the ~3000 km of dextral motion of Gondwana relative to Laurasia in the mid-Permian (Fig. 8), which must have occurred at an average relative plate speed as high as ~15 cm/yr.

The Gondwana/Laurasia transcurrent plate boundary was probably diffuse and the search for possible remnants should focus on mid-Permian shear zones, which may represent reactivation of terminal Variscan shear zones sensu [70]. A possible example is the deep crustal shear synchronous with the emplacement of granitoids (dated at ~280 and ~270 Ma) from the Petite and Grande Kabylie of northern Algeria [71]. The Kabylies, together with Calabria and Corsica-Sardinia, were attached to the French–Catalan margin before the Cenozoic [15]. They were therefore located just where the mid-Permian transformation between Gondwana and Laurasia is expected to have taken place (Fig. 8). To the east of the Kabylies shear system is the Insubric Lineament of northern Adria, which bears evidence of transfer faulting in the Late Paleozoic [72]. To the southeast of Adria, Permian extension is documented in the Ionian basin [73], which was directly linked with the Neotethys Ocean, opening farther to the east between Gondwana and the Cimmerian microcontinents [74].

The geometry of the mid-Permian transcurrent plate boundary, however, can hardly be reconstructed in detail for general reasons given in [75]. Permian wrench lineaments and failed rift arms associated with Pangea transformation were widely reactivated and exploited during the opening of the Jurassic branches of the Neotethys, from the Owen-Somali Basin between Africa/Arabia and India/Madagascar [46] to the Ligurian-Piedmont Ocean [48,49].

9.1. The Variscan heritage

The mid-Permian transformation from Pangea 'B' to Pangea 'A' postdates the cooling of the

Variscan crust. Spatial coincidence and reactivation of the Variscan suture indicate, however, that lithospheric wrenching associated with the mid-Permian Pangea transformation was favored by the weakened state of the crust after collision of Gondwana with Laurasia in the Carboniferous. High degrees of axial anisotropy characterized the Variscan formation of Pangea 'B', which presumably occurred by oblique convergence of Gondwana and Laurasia via a set of E–W shear systems broadly confined between the Uralian front to the east and the Appalachian front to the west [70]. The Variscan Orogen of France and Iberia developed during the Late Paleozoic in a dextral transpressional regime [76]. In the Pyrenees, the Late Paleozoic 'D2' tectonic phase bears ubiquitous evidence of dextral shear associated with the emplacement of syn-tectonic intrusions [77,78]. Additional thermal weakening was related to superplume activity at Kiaman reverse superchron times [79], which may have fostered both Neotethys opening [80] and widespread magmatism in northern and central Europe, the Mediterranean region, and northern Africa [38,81].

10. Conclusions

The following conclusions can be drawn from this study:

1. high quality paleomagnetic data from well-dated volcanic rocks from Gondwana and Laurasia support Pangea 'B' in the Early Permian (Fig. 8);
2. zonal octupole field contamination [6,7] and/or inclination error in sediments [5], if present, cannot rule out the paleomagnetic evidence for Pangea 'B' in the Early Permian. In fact, there is no need to abandon the geocentric axial dipole field model, which has served as working hypothesis for virtually all paleogeographic reconstructions using paleomagnetic data;
3. we accept Pangea 'B' as a valid explanation for Gondwana vs. Laurasia paleomagnetic data and describe a plausible geologic scenario in which the transformation of Pangea occurred from a 'B' configuration in the Early Permian to a Wegenerian-'A' configuration by the end of the Late Permian (Fig. 8). The transformation occurred at a relative plate speed of ~15 cm/yr. No Triassic transformation [2,4] is herein envisaged;
4. the transformation from Pangea 'B' to Pangea 'A' occurred well after Variscan cooling and was probably facilitated by the high anisotropy of the Variscan belt;
5. the transformation from Pangea 'B' to Pangea 'A' is closely associated with the opening of the Neotethys Ocean in the east between India/Arabia and the Cimmerian microcontinents, and widespread lithospheric wrenching and magmatism in the west along the margin of Adria, the African promontory;
6. grand scale plate boundaries and driving forces are qualitatively consistent with a motion of Gondwana to the west relative to Laurasia during the mid-Permian;
7. transcurrent plate boundaries associated with Pangea transformation reactivated older Variscan shear zones [70] and were subsequently exploited by the opening of western Neotethyan seaways in the mid-Jurassic.

Acknowledgements

Rob Van der Voo and an anonymous reviewer made very useful reviews of the manuscript. Edward Irving, David Schelley and Gerard Bossiere made valuable suggestions. LDEO contribution #6513.*[SK]*

References

[1] R. Van der Voo, Paleomagnetism of the Atlantic, Tethys and Iapetus Oceans, Cambridge University Press, Cambridge, 1993, 411 pp.
[2] E. Irving, Drift of the major continental blocks since the Devonian, Nature 270 (1977) 304–309.
[3] G. Muttoni, D.V. Kent, J.E.T. Channell, Evolution of Pangea: Paleomagnetic constraints from the Southern Alps, Italy, Earth Planet. Sci. Lett. 140 (1996) 97–112.
[4] F. Torcq, J. Besse, D. Vaslet, J. Marcoux, L.E. Ricou, M. Halawani, M. Basahel, Paleomagnetic results from Saudi Arabia and the Permo-Triassic Pangea configuration, Earth Planet. Sci. Lett. 148 (1997) 553–567.

[5] P. Rochette, D. Vandamme, Pangea B; an artifact of incorrect paleomagnetic assumptions?, Ann. Geofis. 44 (2001) 649–658.
[6] R. Van der Voo, T.H. Torsvik, Evidence for late Paleozoic and Mesozoic non-dipole fields provides an explanation for the Pangea reconstruction problems, Earth Planet. Sci. Lett. 187 (2001) 71–81.
[7] T.H. Torsvik, R. Van der Voo, Refining Gondwana and Pangea palaeogeography: estimates of Phanerozoic non-dipole (octupole) fields, Geophys. J. Int. 151 (2002) 771–794.
[8] M.W. McElhinny, P.L. McFadden, Paleomagnetism Continents and Oceans, Academic Press, New York, 2000, 386 pp.
[9] J.E.T. Channell, Palaeomagnetism and palaeogeography of Adria, in: A. Morris, D.H. Tarling (Eds.), Palaeomagnetism and Tectonics of the Mediterranean Region, Geol. Soc. London Spec. Publ. 105 (1996) 119–132.
[10] N. Merabet, H. Bouabdallah, B. Henry, Paleomagnetism of the Lower Permian redbeds of the Abadla Basin (Algeria), Tectonophysics 293 (1998) 127–136.
[11] M. Mattei, R. Funicello, C. Kissel, Paleomagnetic and structural evidence for Neogene block rotations in the Central Apennines, Italy, J. Geophys. Res 100 (1995) 17863–17883.
[12] J.E.T. Channell, B. D'Argenio, F. Horvath, Adria, the African promontory, in Mesozoic Mediterranean palaeogeography, Earth Sci. Rev. 15 (1979) 213–292.
[13] W. Lowrie, Paleomagnetism and the Adriatic promontory: a reappraisal, Tectonics 5 (1986) 797–8807.
[14] G. Muttoni, E. Garzanti, L. Alfonsi, S. Cirilli, D. Germani, W. Lowrie, Motion of Africa and Adria since the Permian: paleomagnetic and paleoclimatic constraints from northern Libya, Earth Planet. Sci. Lett. 192 (2001) 159–174.
[15] J.F. Dewey, M.L. Helman, E. Turco, D.H.W. Hutton, S.D. Knott, Kinematics of the western Mediterranean, in: M.P. Coward, Dietrich, D., Park, R.G. (Eds.), Alpine Tectonics, Geol. Soc. London Spec. Publ. 45 (1989) 265–283.
[16] J.S. Oldow, L. Ferranti, D.S. Lewis, J.K. Campbell, B. D'Argenio, R. Catalano, G. Pappone, L. Carmignani, P. Conti, C.L.V. Aiken, Active fragmentation of Adria, the North African promontory, central Mediterranean Orogen, Geology 30 (2002) 779–782.
[17] G. Muttoni, L. Lanci, A. Argnani, A.M. Hirt, U. Cibin, N. Abrahamsen, W. Lowrie, Paleomagnetic evidence for a Neogene two-phase counterclockwise tectonic rotation in the Northern Apennines (Italy), Tectonophysics 326 (2000) 241–253.
[18] J. Besse, V. Courtillot, Revised and synthetic apparent polar wander paths of the African, Eurasian, North American and Indian Plates, and true polar wander since 200 Ma, J. Geophys. Res. 96 (1991) 4029–4050.
[19] R.B. Hargraves, Paleomagnetism of Mesozoic kimberlites in southern Africa and the Cretaceous apparent polar wander curve for Africa, J. Geophys. Res. 94 (1989) 1851–1866.
[20] M.C. Van Fossen, D.V. Kent, A palaeomagnetic study of 143 Ma kimberlite dikes in central New York State, Geophys. J. Int. 113 (1993) 175–185.
[21] A. Castellarin, L. Cantelli, Neo-Alpine evolution of the Southern Eastern Alps, J. Geodyn. 30 (2000) 251–274.
[22] A. Boriani, E. Giobbi Origoni, L. Pinarelli, Paleozoic evolution of southern Alpine crust (northern Italy) as indicated by contrasting granitoid suites, Lithos 35 (1995) 47–63.
[23] G. Cassinis, M. Avanzini, L. Cortesogno, G. Dallagiovanna, P. Di Stefano, L. Gaggero, M. Gullo, F. Massari, C. Neri, A. Ronchi, S. Seno, M. Vanossi, C. Venturini, Synthetic Upper Palaeozoic correlation charts of selected Italian areas, Atti Ticin. Sci. Terra 40 (1998) 65–120.
[24] L. Cortesogno, G. Cassinis, G. Dallagiovanna, L. Gaggero, G. Oggiano, A. Ronchi, S. Seno, M. Vanossi, The Variscan post-collisional volcanism in Late Carboniferous-Permian sequences of Ligurian Alps, Southern Alps and Sardinia (Italy): a synthesis, Lithos 45 (1998) 305–328.
[25] H. Voshage, A.W. Hofmann, M. Mazzucchelli, G. Rivalenti, S. Sinigoi, I. Raczek, G. Demarchi, Isotopic evidence from the Ivrea Zone for a hybrid lower crust formed by magmatic underplating, Nature 347 (1990) 731–736.
[26] L. Pinarelli, A. Del Moro, A. Boriani, V. Caironi, Sr, Nd isotope evidence for an enriched mantle component in the origins of Hercynian gabbro-granite series of the 'Serie dei Laghi' (Southern Alps, NW Italy), Eur. J. Mineral. 14 (2002) 403–415.
[27] S. Martin, M. Zattin, A. Del Moro, P. Macera, Chronologic constraints for the evolution of the Giudicarie belt (Eastern Alps, NE Italy), Ann. Tecton. 10 (1996) 60–79.
[28] U. Schaltegger, P. Brack, Extension and post-orogenic magmatism in the Permian of the Southern Alps: constraints from U, Pb and Hf isotopes, in preparation.
[29] W. Jongmans, Die Karbonflora der Schweiz, Beitr. Geol. Karte Schweiz NF 108 (1960) 97.
[30] M. Menning, A Permian Time Scale 2000 and correlation of marine and continental sequences using the Illawarra Reversal (265 Ma), Nat. Brescia. 25 (2001) 355–362.
[31] H.J. Mauritsch, M. Becke, A magnetostratigraphic profile in the Permian (Groeden Beds, Val Gardena Formation) of the Southern Alps near Paulano (Carnic Alps, Friuli, Italy), Newsl. IGCP Proj. 55 (1983) 80–86.
[32] J.L. Kirschvink, The least-squares line and plane and the analysis of palaeomagnetic data, Geophys. J. R. Astron. Soc. 62 (1980) 699–718.
[33] W. Lowrie, Identification of ferromagnetic minerals in a rock by coercivity and unblocking temperature properties, Geophys. Res. Lett. 17 (1990) 159–162.
[34] L. Tauxe, G.S. Watson, The fold test: an eigen analysis approach, Earth Planet. Sci. Lett. 122 (1994) 331–341.
[35] L. Daly, J.-P. Pozzi, Résultats paléomagnétiques du Permien inférieur et du Trias Marocain; comparaison avec les données Africaines et Sud Americaines, Earth Planet. Sci. Lett. 29 (1976) 71–80.

[36] M. Westphal, R. Montigny, R. Thuizat, C. Bardon, A. Bossert, R. Hamzeh, Paléomagnétisme et datation du volcanisme permien, triasique et crétace du Maroc, Can. J. Earth Sci. 16 (1979) 2150–2164.
[37] A. Saidi, A. Tahiri, L. Ait Brahim, M. Saidi, States of stresses and opening/closing mechanisms of the Permian basins in Hercynian Morocco. The example of the Jebilet and Rehamna Basins, C. R. Geosci. 334 (2002) 221–226.
[38] R. Benek, W. Kramer, T. McCann, M. Scheck, J.F.W. Negendank, D. Korich, H.-D. Huebscher, U. Bayer, Permo-Carboniferous magmatism of the Northeast German Basin, Tectonophysics 266 (1996) 379–404.
[39] R. Van der Voo, R.B. French, Apparent polar wandering for the Atlantic-bordering continents: Late Carboniferous to Eocene, Earth Sci. Rev. 10 (1974) 99–119.
[40] E. Garzanti, D. Sciunnach, Early Carboniferous onset of Gondwanan glaciation and Neo-Tethyan rifting in Southern Tibet, Earth Planet. Sci. Lett. 148 (1997) 359–365.
[41] J. Al-Belushi, K.W. Glennie, B.P.J. Williams, Permo-Carboniferous glaciogenic Al Khlata Formation, Oman: A new hypothesis for origin of its glaciation, Geo-Arabia 1 (1996) 389–403.
[42] L. Spring, F. Bussy, J.-C. Vannay, S. Huon, M.A. Cosca, Early Permian granitic dykes of alkaline affinity in the Indian High Himalaya of Upper Lahul and SE Zanskar: geochemical characterization and geotectonic implications, in: P.J. Treloar, M.P. Searle (Eds.), Himalayan Tectonics, Geol. Soc. London Spec. Publ. 74 (1993) 251–264.
[43] V. Caironi, E. Garzanti, D. Sciunnach, Typology of detrital zircon as a key to unravelling provenance in rift siliciclastic sequences (Permo-Carboniferous of Spiti, N India), Geodin. Acta 9 (1996) 101–113.
[44] E. Garzanti, L. Angiolini, D. Sciunnach, The mid-Carboniferous to lowermost Permian succession of Spiti (Po Group and Ganmachidam Fm.; Tethys Himalaya, Northern India): Gondwana glaciation and rifting of Neo-Tethys, Geodin. Acta 9 (1996) 78–100.
[45] E. Garzanti, Stratigraphy and sedimentary history of the Nepal Tethys Himalayan passive margin, J. Asian Earth Sci. 17 (1999) 805–827.
[46] L. Angiolini, M. Balini, E. Garzanti, A. Nicora, A. Tintori, Gondwanan deglaciation and opening of Neotethys: the Al Khlata and Saiwan Formations of Interior Oman, Palaeogeogr. Palaeoclimatol. Palaeoecol. 196 (2003) 99-123.
[47] G.B. Piccardo, E. Rampone, R. Vannucci, F. Cimmino, Upper mantle evolution of ophiolitic peridotites from the Northern Apennine: petrological constraints to the geodynamic processes, Mem. Soc. Geol. It. 48 (1994) 137–148.
[48] M. Marroni, G. Molli, A. Montanini, R. Tribuzio, The association of continental crust rocks with ophiolites in the Northern Apennines (Italy): implications for the continent-ocean transition in the Western Tethys, Tectonophysics 292 (1998) 43–66.
[49] V. Trommsdorff, J. Hermann, O. Muentener, M. Pfiffner, A.C. Risold, Geodynamic cycles of subcontinental lithosphere in the Central Alps and the Arami enigma, J. Geodyn. 30 (2000) 77–92.
[50] A. Montanini, R. Tribuzio, Gabbro-derived granulites from the Northern Apennines (Italy): Evidence for lower-crustal emplacement of tholeiitic liquids in post-Variscan times, J. Petrol. 42 (2001) 2259–2277.
[51] F. Bussy, G. Venturini, J. Hunziker, G. Martinotti, U-Pb ages of magmatic rocks of the western Austroalpine Dent-Blanche-Sesia unit, Schweiz. Mineral. Petrogr. Mitt. 78 (1998) 163–168.
[52] W. Hansmann, O. Müntener, J. Hermann, U-Pb zircon geochronology of a tholeitic intrusion and associated migmatites at a continental crust-mantle transition, Val Malenco, Italy, Schweiz. Mineral. Petrogr. Mitt. 81 (2001) 239–255.
[53] A. Mayer, K. Mezger, S. Sinigoi, New Sm ± Nd ages for the Ivrea Verbano Zone, Sesia and Sessera valleys (Northern-Italy), J. Geodyn. 30 (2000) 147–166.
[54] C. Pin, Datation U-Pb sur zircons à 285 M.a. du complexe gabbro-dioritique du Val Sesia-Val Mastallone et âge tardi-hercynien du métamorphisme granulitique de la zone Ivrea-Verbano (Italie), C. R. Acad. Sci. Paris 303 (1986) 827–829.
[55] A. Rottura, G.M. Bargossi, A. Caggianelli, A. Del Moro, D. Visonà, C.A. Tranne, Origin and significance of the Permian high-K calc-alkaline magmatism in the central-eastern Southern Alps, Italy, Lithos 45 (1998) 329–348.
[56] M.R. Handy, J.E. Streit, Mechanics and mechanisms of magmatic underplating: inferences from mafic veins in deep crustal mylonite, Earth Planet. Sci. Lett. 165 (1999) 271–286.
[57] E. Pandeli, G. Gianelli, M. Puxeddu, F.M. Elter, The Paleozoic basement of the Northern Apennines: stratigraphy, tectono-metamorphic evolution and alpine hydrothermal processes, Soc. Geol. It. Mem. 48 (1994) 627–654.
[58] G. Gosso, G.B. Siletto, M.I. Spalla, H-T/L-P metamorphism and structures in the South-Alpine basement near Lake Como, Orobic Alps: intracontinental imprints of the Permo-Triassic rifting, Ofioliti 22 (1997) 133–145.
[59] M. Thöni, A review of geochronological data from the Eastern Alps, Schweiz. Mineral. Petrogr. Mitt. 79 (1999) 209–230.
[60] G. Rebay, M.I. Spalla, Emplacement at granulite facies conditions of the Sesia-Lanzo metagabbros: an early record of Permian rifting?, Lithos 58 (2001) 85–104.
[61] D. Sciunnach, E. Garzanti, M. Confalonieri, Stratigraphy and petrography of Upper Permian to Anisian terrigenous wedges (Verrucano Lombardo, Servino and Bellano Formations; western Southern Alps), Riv. It. Paleontol. Stratigr. 102 (1996) 27–48.
[62] F. Massari, C. Neri, The infill of a supradetachment(?) basin: the continental to shallow-marine upper Permian succession in the Dolomites and Carnia (Italy), Sediment. Geol. 110 (1997) 181–221.
[63] E. Garzanti, L. Angiolini, D. Sciunnach, The Permian Kuling Group (Spiti, Lahaul and Zanskar; NW Hima-

laya): sedimentary evolution during rift/drift transition and initial opening of Neo-Tethys, Riv. It. Paleontol. Stratigr. 102 (1996) 175–200.
[64] A.A. Al-Aswad, Stratigraphy, sedimentary environment and depositional evolution of the Khuff Formation in south-central Saudi Arabia, J. Pet. Geol. 20 (1997) 307–326.
[65] L. Angiolini, M. Balini, S. Crasquin, E. Garzanti, G. Muttoni, A. Nicora, A. Tintori, Permian climatic and palaeogeographic changes in Northern Gondwana: the Khuff Fm. of the Haushi-Huqf (Oman), Palaeogeogr. Palaeoclimatol. Palaeoecol. 191 (2003) 269–300.
[66] M. Gaetani et al., Wordian paleogeographic map, in: J. Dercourt, M. Gaetani et al. (Eds.), Peri-Tethys Atlas and Explanatory Notes, vol. 3 (2001) 19–25.
[67] H. Stollhofen, B. Frommherz, I.G. Stanistreet, Volcanic rocks as discriminants in evaluating tectonic versus climatic control on depositional sequences, Permo-Carboniferous continental Saar-Nahe Basin, in: H.M. Pedley, L.E. Frostick (Eds.), Unravelling Tectonic and Climatic Signals in Sedimentary Successions, J. Geol. Soc. London 156 (1999) 801–808.
[68] T. McCann, The Rotliegend of the NE German Basin: background and prospectivity, Pet. Geosci. 4 (1998) 17–27.
[69] C. Scotese, Atlas of Earth History, PALEOMAP Project, Arlington, TX, 2001, 52 pp.
[70] F. Arthaud, P. Matte, Late Paleozoic strike-slip faulting in southern Europe and northern Africa: Result of a right-lateral shear zone between the Appalachians and the Urals, Geol. Soc. Am. Bull. 88 (1977) 1305–1320.
[71] J.J. Peucat, Y. Mahdjoub, A. Drareni, U-Pb and Rb-Sr geochronological evidence for late Hercynian tectonic and Alpine overthrusting in Kabylian metamorphic basement massifs (northeastern Algeria), Tectonophysics 258 (1996) 195–213.
[72] K.H. Brodie, D. Rex, E.H. Rutter, On the age of deep crustal extensional faulting in the Ivrea Zone, northern Italy, in: M.P. Coward, D. Dietrich, R.G. Park (Eds.), Alpine Tectonics, Geol. Soc. London Spec. Publ. 45 (1989) 203–210.
[73] S. Merlini, G. Cantarella, C. Doglioni, On the seismic profile CROP M5 in the Ionian Sea, Boll. Soc. Geol. It. 119 (2000) 227–236.
[74] P.A. Ziegler, G.M. Stampfli, Late Palaeozoic-Early Mesozoic plate boundary reorganization: collapse of the Variscan Orogen and opening of Neotethys, Nat. Brescia. 25 (2001) 17–34.
[75] P.J. Umhoefer, Where are the missing faults in translated terranes?, Tectonophysics 326 (2000) 23–35.
[76] D. Shelley, G. Bossiere, A new model for the Hercynian Orogen of Gondwanan France and Iberia, J. Struct. Geol. 22 (2000) 757–776.
[77] G. Gleizes, D. Leblanc, J.L. Bouchez, The main phase of the Hercynian Orogeny in the Pyrenees is a dextral transpression, Geol. Soc. Spec. Publ. 135 (1998) 267–273.
[78] E. Druguet, D.H.W. Hutton, Syntectonic anatexis and magmatism in a mid-crustal transpressional shear zone; an example from the Hercynian rocks of the eastern Pyrenees, J. Struct. Geol. 20 (1998) 905–916.
[79] R.L. Larson, Geological consequences of superplumes, Geology 19 (1991) 963–966.
[80] E. Garzanti, Himalayan ironstones, 'superplumes', and the breakup of Gondwana, Geology 21 (1993) 105–108.
[81] M. Doblas, R. Oyarzun, J. Lopez-Ruiz, J.M. Cebria, N. Youbi, V. Mahecha, M. Lago, A. Pocovi, B. Cabanis, Permo-Carboniferous volcanism in Europe and northwest Africa: a superplume exhaust valve in the centre of Pangaea?, J. Afr. Earth Sci. 26 (1998) 88–99.
[82] B.R. Wardlaw, T.A. Schiappa, Toward a refined Permian chronostratigraphy, in: G. Cassinis (Ed.), Permian Continental Deposits of Europe and Other Areas. Regional Reports and Correlations, Nat. Brescia. Monogr. 25 (2001) 363–365.
[83] R. Mundil, I. Metcalfe, K.R. Ludwig, P.R. Renne, F. Oberli, R.S. Nicoll, Timing of the Permian-Triassic biotic crisis: implications from new zircon U/Pb age data (and their limitations), Earth Planet. Sci. Lett. 187 (2001) 131–145.
[84] I. Metcalfe, R.S. Nicoll, R. Mundil, C. Foster, J. Glen, J. Lyons, W. Xiaofeng, W. Cheng-yuan, P.R. Renne, L. Black, Q. Xun, M. Xiadong, The Permian-Triassic boundary and mass extinction in China, Episodes 24 (2001) 239–244.
[85] A.L. Lottes, D.B. Rowley, Reconstruction of the Laurasian and Gondwanan segments of Permian Pangaea, in: W.S. McKerrow, C.R. Scotese (Eds.), Palaeozoic Palaeogeography and Biogeography, Geol. Soc. Am. Mem. 12 (1990) 383–395.
[86] E.C. Bullard, J.E. Everett, A.G. Smith, A symposium on continental drift. IV. The fit of the continents around the Atlantic, Phil. Trans. R. Soc. London A 258 (1965) 41–51.

Available online at www.sciencedirect.com
SCIENCE DIRECT®
ELSEVIER
Earth and Planetary Science Letters 6934 (2003) 1–2
EPSL
www.elsevier.com/locate/epsl

Erratum

Erratum to "Early Permian Pangea 'B' to Late Permian Pangea 'A'"[Earth Planet. Sci. Lett. 215 (2003) 379–394]☆

Giovanni Muttoni [a,*], Dennis V. Kent [b,c], Eduardo Garzanti [d], Peter Brack [e], Niels Abrahamsen [f], Maurizio Gaetani [a]

[a] *Dipartimento di Scienze della Terra, Università di Milano, via Mangiagalli 34, 20133 Milan, Italy*
[b] *Lamont-Doherty Earth Observatory, Palisades, NY 10964, USA*
[c] *Department of Geological Sciences, Rutgers University, Piscataway, NJ 08854, USA*
[d] *Dipartimento di Scienze Geologiche e Geotecnologie, Università di Milano-Bicocca, Piazza della Scienza 4, 20126 Milan, Italy*
[e] *Departement Erdwissenschaften, ETH-Zentrum, CH-8092 Zürich, Switzerland*
[f] *Department of Earth Sciences, Aarhus University, Aarhus, Denmark*

In the above article there was an error in Fig. 3. The correct figure is printed below. The publisher would like to apologize for any inconvenience caused.

☆ doi: of original article 10.1016/S0012-821X(03)00452-7.

* Corresponding author. Tel.: +39-02-503-15518; Fax: +39-02-503-15494.
E-mail address: giovanni.muttoni1@unimi.it (G. Muttoni).

0012-821X/03/$ – see front matter
doi:10.1016/S0012-821X(03)00660-5

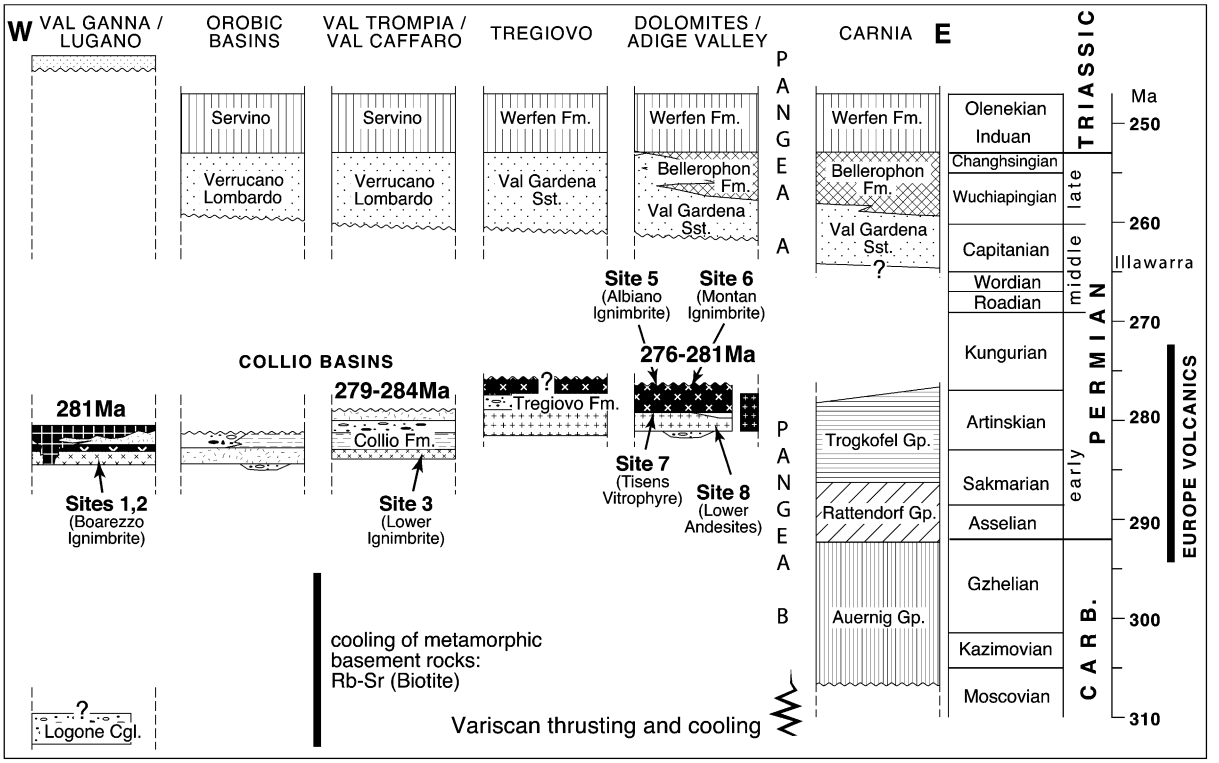

Fig. 3. Age and stratigraphy of Permian units in the Southern Alps with indication of sampling sites. The Permian part of this time scale is a close derivative of [82] with a modified age for the base of the Triassic after [83,84]. For the age of the Upper Carboniferous, we followed [30]. Range of cooling ages for the upper crustal basement of the Southern Alps is after [27,28].